

Definitions of state variables and state space for brain-computer interface

Part 1. Multiple hierarchical levels of brain function

Walter J Freeman
Department of Molecular & Cell Biology
University of California at Berkeley
Berkeley CA 94720-3206 USA
<http://sulcus.berkeley.edu>
dfreeman@berkeley.edu

Invited review: **Cognitive Neurodynamics** 1(1): 3-14
<http://dx.doi.org/10.1007/s11571-006-9001-x>

Key words: beta activity β ; BCI; BMI; electrocorticogram ECoG; epsilon activity ϵ ; gamma activity γ ; intentional action; local field potential LFP; multiple spike activity MSA; multiunit activity MUA; state variables; state transitions

30 July 2006

23 Pages

9,710 words

2 Figures

1 Appendix

Acknowledgment

I am grateful for permission from J. C. Sanchez, Department of Pediatrics, Division of Neurology, and P. C. Carney and J. C. Principe, Department of Electrical and Computer Engineering, University of Florida, Gainesville FL 32611 to use their figure illustrating intracranial recording.

Abstract

Neocortical state variables are defined and evaluated at three levels: microscopic using multiple spike activity (MSA), mesoscopic using local field potentials (LFP) and electrocorticograms (ECoG), and macroscopic using electroencephalograms (EEG) and brain imaging. Transactions between levels occur in all areas of cortex, upwardly by integration (abstraction, generalization) and downwardly by differentiation (speciation). The levels are joined by circular causality: microscopic activity upwardly creates mesoscopic order parameters, which downwardly constrain the microscopic activity that creates them. Integration dominates in sensory cortices. Microscopic activity evoked by receptor input in sensation induces emergence of mesoscopic activity in perception, followed by integration of perceptual activity into macroscopic activity in concept formation. The reverse process dominates in motor cortices, where the macroscopic activity embodying the concepts supports predictions of future states as goals. These macroscopic states are conceived to order mesoscopic activity in patterns that constitute plans for actions to achieve the goals. These planning patterns are conceived to provide frames in which the microscopic activity evolves in trajectories that adapted to the immediate environmental conditions detected by new stimuli. This circular sequence forms the action-perception cycle. Its upward limb is understood through correlation of sensory cortical activity with behavior. Now brain-machine interfaces (BMI) offer a means to understand the downward sequence through correlation of behavior with motor cortical activity, beginning with macroscopic goal states and concluding with recording of microscopic MSA trajectories that operate neuroprostheses. Part 1 develops a hypothesis that describes qualitatively the neurodynamics that supports the action-perception cycle and derivative reflex arc. Part 2 describes episodic, "cinematographic" spatial pattern formation and predicts some properties of the macroscopic and mesoscopic frames by which the embedded trajectories of the microscopic activity of cortical sensorimotor neurons might be organized and controlled.

1. Introduction to BCI

The brain-computer interface (BCI) or brain-machine interface (BMI) begins with attachment of electrodes in or near the brain to measure and model its electrical activity. Direct control by means of brain electrical activity of an instrument for communication by a victim of paralysis or a remote platform by a scientist wanting to explore an inhospitable environment requires BCI. The first BCI using the scalp EEG (electroencephalogram) for device control was developed by student engineers in Berkeley California in the 1960s soon after the invention of the transistor enabled construction of lightweight, low-power amplifiers, filters, and electronic switches. Users demonstrated remote on-off control of a light, an electric train, or a cursor on a monitor by inducing and blocking alpha waves. Engineers learned to control alpha by means of biofeedback, in which the sub-audible alpha waves (8-12 Hz) were used to modulate a 1 kHz carrier wave in a so-called 'alphaphone', so that one could immediately sense the audible FM or AM tone as an indicator of his or her alpha waves (Millay, 1999). The techniques then were too primitive to achieve more than on-off switching in BCI, but they have flourished in biofeedback (Othmer, Othmer and Kaiser, 1999), especially with evoked potential techniques (Cheng et al., 2002) for single-trial EEG as well (Blankertz et al., 2004). Gao et al. (2003) used steady-state visual evoked potentials giving an information transfer rate up to 68 bits/minute. Even so the baffling complexity of EEG, the smoothing by the impedance barriers of the skull and scalp, and the contamination by noise from muscle and eye movements still severely limit its utility for BCI.

An alternative approach for BCI research is based on the technology for reliable recording of the spike trains of single neurons with arrays of multiple microelectrodes inserted directly into the neocortex of an experimental animal (Georgopoulos, Schwartz and Kettner, 1986; Chapin et al., 1999; Wessburg et al., 2000; Nicolelis, 2001; Serruya et al., 2002; Donoghue, 2002; Taylor et al., 2002; Kipke, Vetter and Williams, 2003; Sanchez et al., 2004; Musallam et al., 2004; Andersen et al., 2004). Bundles of very fine wires (25-100 micron diameter) are inserted into the deeper layers of the frontal and parietal cortices that include the sensorimotor cortex of a monkey or a rat. The locations of the tips of the wires are adjusted to isolate the spike trains of multiple neurons from each tip (Nicolelis, 2003). Alternatively spikes are recorded from a silicon probe inserted vertically through a single cortical hypercolumn spanning 2 mm with spikes recorded at 50 micron intervals (Blanche et al., 2005; Hochberg et al., 2006). The spikes from single neurons are identified by pattern recognition algorithms of the spike waveforms sampled at rates 10-40 kHz (spike durations are typically ~ 1 ms) and digitized as 1's for spikes in sequences of 0's for each identified neural spike train. The animal is trained to use a forelimb to move a lever in order to get a reward (typically juice to slake thirst). The spike trains are binned into sets of spatiotemporal feature vectors of multiple spike activity (MSA) in steps typically of 50-250 ms. After the animal has learned the task, the feature vectors are used instead of the limb movement to control an electronic switch that delivers the

reward. For a while the animal continues to use the lever despite the disconnect. Eventually the lever is removed, and the animal receives the reward solely by generating the spike trains.

The amount of information in the MSA integrated over many trials suffices to replicate 80% of the variance in the trajectory of limb movement needed to press the lever, and to decompose the feature vectors that capture the contributions of different spike trains to each stage of movement (Carmena et al., 2003). The high variability of the spike trains is dealt with by spatiotemporal averaging through a linear regressor (FIR adaptive filter), indicating that the information used by the brain for lever control is distributed over many neurons (Lee et al., 1998; Cohen and Nicolelis, 2004; DiGiovanna, Sanchez and Principe, 2006). On the one hand investigators can demonstrate control of simple movements by as few as 7-16 neurons (Seruya et al., 2002), and on the other hand the reliability and complexity of control can be enhanced by using as many spikes in MSA as can be extracted, already exceeding 100 sampled neural spike trains (Nicolelis, 2001; Carmena et al., 2005; Blanche et al., 2005) but with diminishing returns for with increasing numbers by standard adaptive filtering techniques (Sanchez et al., 2006). With further improvements in the engineering techniques this form of BCI may achieve use of cortical action potentials for control of more complex actions. However, use of this technique for BCI in human subjects is restricted to hospitalized victims of global paralysis such as the ‘locked-in syndrome’ (Hinterberger et al., 2003), for whom communication and environmental engagement by this method requires surgical invasion for BCI, with poor prospects for long term stability in a clinical setting (Hochberg et al., 2006). Moreover, sampling with microelectrodes is constrained to recording spike trains from at most 10^3 neurons, which are embedded in cortex containing 10^5 neurons/mm³, and which are distributed over areas exceeding 10^3 mm³, suggesting sample rates less than 1 neuron in 10^5 by use of microelectrodes. In effect, greater information transfer rates are needed to construct a variety of limb trajectories for flexible BCI. Scalp EEG may meet that need when its mechanisms are adequately understood.

2. Definitions of state variables and state space at three hierarchical levels

The control of limb movement depends on sequential patterns of brain activity that are indirectly observed by recording the extracellular potential differences created by loop currents of neurons. The loop currents are the basis for observing the electric potentials of both the spikes of axons and the dendritic currents by which spikes are controlled, all of which sum in the volume conductor of the whole brain. The voltage of each sequential pattern oscillates at a characteristic frequency that carries a spatial pattern by amplitude and phase modulation. A pattern that lasts at least three to five cycles at the characteristic frequency is called a frame. The frame defines a brain state that emerges by a state transition and collapses by another state transition to a new pattern. Such conditionally stable patterns were described by Ilya Prigogine (1980) in terms of the emergence of order from disorder by formation of “dissipative structures” [patterns in

frames], and by Hermann Haken (1983) in terms of “order parameters” [patterns in frames] of ensembles that constrain the particles creating them. During the state transitions the brain is referred to as metastable (Bressler and Kelso, 2001; Fingelkurts and Fingelkurts, 2004). The full description of a sequence of brain states includes not only the patterns but also the behavior, the brain modules (Houk, 2005) that control behavior, and the context in which the brain is planning, predicting and evaluating the behavior (Houk and Wise, 1995; Andersen et al., 2004).

A set of signals from an array of n electrodes determines a set of n state variables and the dimensions of their n -space (Freeman, 1975/2004, 2005a; Basar, 1998; Sanchez et al., 2006). The n -space is a finite subspace projected from the essentially infinite state space of the brain; each channel defines an independent axis in the state space. The ranges of values taken by the measurements of the electric potentials define the boundaries of the accessible state space. The measurement of the n state variables at one point in time gives a point in n -space. Multiple recurrences by repeated measurement giving nearly the same pattern define a state by a cluster of points. A sequence of points through state space defines a trajectory. The shift by a trajectory from one cluster to another cluster defines a state transition. Each cluster of points manifests a self-organized brain state that is governed by an attractor. Each attractor is surrounded by a basin of attraction, so that when a trajectory crosses into the basin, the brain converges to that pattern. A collection of basins and attractors forms an attractor landscape. A habitual sequence of patterns is connected by a pathway that is called an itinerant trajectory (Tsuda, 2001), in analogy to migrant workers following the seasons. This state-space approach to dynamics gives great flexibility in describing the neural correlates of behaviors, because the clusters of points can be defined at different scales of time and space, and the measured state variables can be processed and combined in many different ways that flexibly reflect the underlying dynamics.

These state variables then may also serve as variables in analytic equations that express the dynamics revealed by data-driven models in nonlinear differential equations (Freeman, 1975/2004) forming K-sets (Kozma and Freeman, 2001; Principe, et al., 2001; Kozma, Freeman and Erdí, 2003; Li et al., 2006) and neuropercolation theory (Kozma et al., 2005). These modeling aspects will not be elaborated here. Instead emphasis is given to the choice of state variables representing brain activity at different scales of time and space. There is increasing evidence that brain dynamics is scale-free (Barabási, 2002), thus accounting for the similarity in temporal dynamics among mammalian species of neocortex (reviewed by Freeman, 2005b) despite its vast range of variation in area (Bok, 1959). Recent ECoG findings have shown the utility of discretizing the continuum into three levels: microscopic (MSA), mesoscopic (LFP and local ECoG) and macroscopic (large-scale ECoG, EEG, and whole brain imaging). Transitions between levels are described in terms of circular causality (Haken, 1983, 2006); ensembles of neurons create mesoscopic order parameters that

regulate the microscopic neurons in the ensembles. In sensory cortices the microscopic input is followed within a few milliseconds by emergence of a sequence of mesoscopic patterns reflecting integration within each primary sensory receiving area (Barrie, Freeman and Lenhart, 1996). Roughly half a second later, multicortical patterns emerge that span much of the cerebral hemisphere (Freeman and Burke, 2003; Freeman and Rogers, 2003) and that reflect macroscopic integration of mesoscopic patterns into a macroscopic pattern that includes both limbic and the primary motor areas (Freeman, 2005a). Hypothetically in premotor and motor cortices this macroscopic goal-state orders and embeds the emergence of mesoscopic states that regulate spike trains of microscopic neurons carrying motor cortical output.

3. Interrelation of state variables; dendritic field potentials and axonal spikes

Brain activity coexists at the three levels, and the observed loop currents from all levels contribute potential differences simultaneously in all of the n channels used for observation. The task of analysis is to decompose them in order to define and measure useful state variables at each level. It is essential to average the data. Two types of averaging are used that extract data structures at different levels. Time averaging across trials removes the background activity as noise and emphasizes the stimulus- or event-related components of the data: macroscopic event-related potentials (ERP) from field potentials and microscopic post stimulus time histograms (PSTH) from MSA. Spatial averaging in single trials over signals from high-density electrode arrays enhances the background activity, making it possible to study its reorganization by state transitions under the impact of stimuli (Freeman, 2004). Spatial averaging gives reference values for phase and amplitude patterns and their rates of change in the spatial and temporal dimensions for every signal that is used to get the spatial average in single trials. The averaged waveforms from field potentials can be decomposed by linear techniques (Freeman, 1975/2004; Nunez et al., 1997; Basar, 1998).

A multi-dimensional approach to BCI is based not only on levels but also on the fact that neurons have two main functional branches. Dendrites receive spikes and sum them by converting the MSA into waves of dendritic current density. Axons transmit spike trains that express magnitudes of dendritic activity by pulse rates and intervals. Dendritic currents regulate spike output at trigger zones and in turn are regulated by spike input at synapses. For single neurons the spike rate has repeatedly been demonstrated to be linearly additive and proportional to transmembrane current density imposed with an intracellular electrode between the limits of threshold and doublet firing over a broad range (e.g., Granit and Renkin, 1961; Granit, Kernell and Shortess, 1963). At synapses the postsynaptic potential amplitude is nonlinear, because the amplitude of the impulse response decreases as the evoked amplitude level approaches the equilibrium potential of the synaptic generator. To the contrary, for a population of neurons the relation of pulse density (MSA amplitude) to mean transmembrane current density (ECoG) is nonlinear but monotonic at trigger zones. Typically the relation is sigmoid (Fig.

1.01), owing to the distributions of thresholds. The relation of pulse density to dendritic wave amplitude at synapses is kept within a narrow near-linear range at synapses (Freeman, 1975/2004).

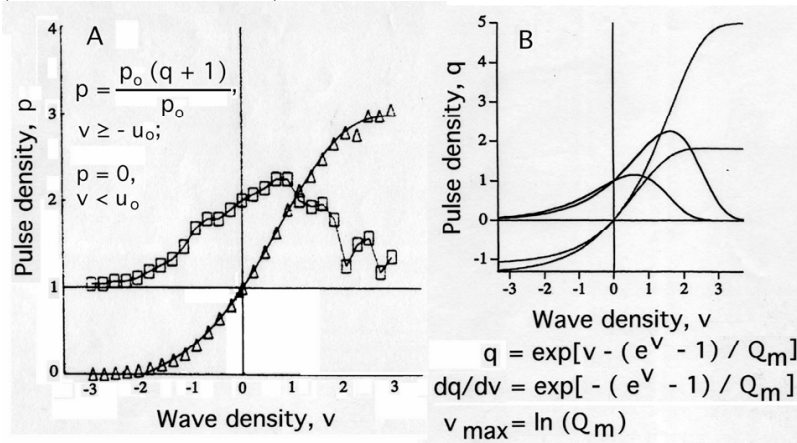


Fig. 1.01. A. Triangles show normalized pulse probability density conditional on wave amplitude from equation (A1.7) in Appendix 1. Squares show the numerical derivative. **B.** The sigmoid equation for the static nonlinear wave-pulse relation is derived by a statistical mechanical generalization from the Hodgkin-Huxley equations. The derivative, dq/dv , gives the forward nonlinear gain. Q_m designates the maximal asymptote, which increases above rest ($Q_m = 2$) with hunger, rage, etc. ($Q_m = 5$). From Freeman (1979)

Synaptic current always flows in closed loops, with the electromotive force located in the high-resistance current source in the synapse, and the maximum energy dissipation at the matching resistance in the axonal trigger zone. Both axonal and synaptic loop currents cause weak fields of electric potential in the extracellular low-resistance volume conductor. They differ from the transmembrane potential differences in two respects. First, they are lower in magnitude by 10^3 owing to the low extraneuronal specific resistance. Second, they result from the sum of extracellular current densities of all participating neurons in the neighborhood, estimated to be conservatively on the order of 10^4 (Sholl, 1956; Bok, 1959; Freeman, 1975/2004; Braitenberg and Schüz, 1998). Therefore axonal pulses are microscopic, and dendritic waves are mesoscopic.

The pervasive background activity observed in BCI is caused by mutual excitation among cortical neurons, predominantly local. About 85% of cortical neurons are pyramidal neurons (Sholl, 1956; Braitenberg and Schüz, 1998). Each excitatory neuron transmits to $\sim 10^4$ other neurons and receives from $\sim 10^4$ other neurons but not the same neurons to which they transmit. The likelihood of any two neurons having a reciprocal connection is about 10^{-6} (Braitenberg and Schüz, 1998; Liley and Wright, 1994). The mutual excitation results in self-sustained 'spontaneous' background activity. That activity is locally stabilized everywhere by the thresholds and refractory periods of axons (Freeman, 1975/2004; 2006). The dynamics is modeled with a 4th order nonlinear differential equation (a KLe set, Freeman, 1975/2004). In the language of linear dynamics, linearization of the equations at the operating point gives a zero eigenvalue that specifies a closed loop pole at the origin of the complex plane. In the language of nonlinear

dynamics, the population maintains a stable, non-zero point attractor. In the language of physics the population maintains a stable ground state. In the language of neurophysiology the population sustains steady-state background activity. Each local neighborhood ('cortical column') has two measurable quantities with mean values that are governed by this attractor: the local mean field dendritic current density and the local axonal pulse density. For an estimate of the average background firing rate of cortical neurons of $\sim 1/s$ (Swadlow, 1994), the average pulse density of 10^4 would be $\sim 10,000$ spikes/s. Each spike lasts about 1 ms, which allows treatment of spike density as a continuous variable with its modulation depth limited by thresholds and refractory periods (Fig. 1.01). In the language of engineering a population signal is formed by time-multiplexing across the 10^4 neurons participating in the mesoscopic pattern.

Wave density is recorded extracellularly as a continuous analog time series before digitizing. The pulse density (at the mesoscopic level) must be computed from an average over MSA. It is not possible to record the spike trains of all 10^4 contributing neurons, so the ergodic hypothesis is invoked. It must be assumed that over a long enough time in the resting state the mesoscopic participation of an observed neuron will occupy the states of all the neurons at any one time, with respect to its contributions to the LFP and ECoG. This assumption holds only for brains at rest or under light anesthesia and does not hold for neurons in brains of animals engaged in intentional behavior or driven in ERP and PSTH. Owing to the nonstationarity of brains repeatedly departing from the rest state the wave-pulse relation of neuron populations can be tested only with individual neurons that have spike rates $\geq 10/s$ in order to get the 10^4 spikes needed in 1,000 s (~ 17 minutes) of recording. More commonly MSA with ~ 10 spike trains giving an average rate of 10/s are used to interrelate MSA and LFP or ECoG.

The statistical wave-pulse relation (Appendix 1) at trigger zones of axons is expressed in a sigmoid curve as the probability of pulse occurrence conditional on wave amplitude (Fig. 1.01, triangles calculated with equation (A1.7)). The amplitude histograms of LFP and ECoG typically are Gaussian. The distributions of interspike intervals of the single spike trains typically conform to a Poisson process with a dead time (the refractory periods) and the correlations between spike trains are very low (Abeles, 1991). The spectrum of MSA (300-6000 Hz) tends to be flat resembling white noise ($1/f^0$), while the spectrum of field potentials tends to resemble "brown" noise ($1/f^2$) (Schroeder, 1991). The impulse response of a mutually excitatory population to single shock stimuli shows a brief oscillation at high frequency (80-250 Hz, the epsilon range) in the field potential accompanied by chattering of single cells at spike intervals $\sim 4-5$ ms followed by exponential decay back to the baseline.

These properties are readily simulated with a random number generator, provided that the flat spectrum ($1/f^0$) is weighted by a $1/f^2$ filter:

$$A^2(f) = -2 \text{ antilog}_{10}(a(f)),$$

where f is frequency in Hz, a is the noise amplitude before filtering, and A is noise power after filtering (Freeman, 2006), which reflects the way in which the background activity is generated (Ch. 8 in Freeman, 2000) by summation of innumerable random processes (p. 125 in Schroeder, 1991) in mutual excitation. Each neuron is multitasking; it contributes specifically to its local networks at the microscopic level, and simultaneously it interacts with its neighborhood and participates at the population level with a small fraction of the variance of its pulse train by time-multiplexing (rotating at random among neurons the duty of transmitting a spike while maintaining a high transmission pulse density with low spatial density). That small fraction of the variance of its pulse train is not detectable in an isolated single microscopic pulse train, yet it contributes to the mesoscopic state variable of the neighborhood. The transfer function for the feedback pathway of each neuron with its neighborhood can be approximated by a one-dimensional diffusion process with a lumped delay, T , for which the transfer function in a piece-wise linear approximation is $\exp(-(sT)^{0.5})$ (Freeman, 1975/2004) that randomizes spike occurrences and likewise the refractory periods on each passage around the positive feedback loop between each neuron and its local neighborhood. Hence the nonlinear relation between microscopic spikes and mesoscopic waves can be treated as static rather than dynamic, in contrast to the time-varying nonlinear dynamics of single neurons described by the Hodgkin-Huxley equations, which relate lower level kinetics of ions and ion channels to higher level membrane currents.

The extraneuronal dendritic potential recorded from the same depth electrode as the MSA is the LFP. Each electrode samples the LFP over multiple neural populations comprising multiple cortical hypercolumns, each on the order of 1.0 mm in diameter containing $\sim 10^5$ neurons/mm³; though the radius of spike detection is commonly asserted to be roughly 200 microns, the radius for detection of LFP components is undefined and well exceeds 1 mm. An array of 10^2 electrodes sampling the mean fields of an area of cortex 10x10 mm (Freeman et al., 2000) might in theory give sampling averaging 1 neuron in 10, an improvement over 1 in 10^5 . Further, the dendritic current of the LFP spreads by volume conduction (Nunez et al., 1997) to the pial surface of the cortex, where it gives the electrocorticogram (ECoG) without need for penetration into the cortex (Fig. 1.02). The current also spreads to the overlying scalp giving the EEG. These features indicate that wave recording might surmount the sampling limitations on spike recording, as suggested also by Mehring et al. (2003) despite the complexities of the relations between MSA and LFP Wang et al. (2006).

However, there remains a long and arduous path from single neuron recording through LFP and ECoG to the EEG as a channel for BCI. The key point here is that the farther one places the recording electrode from the generating cortex, the greater is the loss of detail by spatiotemporal smoothing. Yet the brain is doing exactly that — spatial averaging — prior to constructing its motor control patterns in self-organization of the activity of billions of neurons. Likewise researchers are averaging their MSA data, often to find oscillations in firing probabilities. Reports

of gamma scalp EEG correlates of behavior are now commonplace (Müller et al., 1996; Tallon-Beaudry et al., 1996, 1998; Rodriguez et al., 1999; Miltner et al., 1999), as well as reports of epsilon correlates (Gonzalez et al., 2006), which demonstrate the enhancement of global ECoG signals by smoothing that may enable researchers, metaphorically speaking, to see the forest instead of the trees.

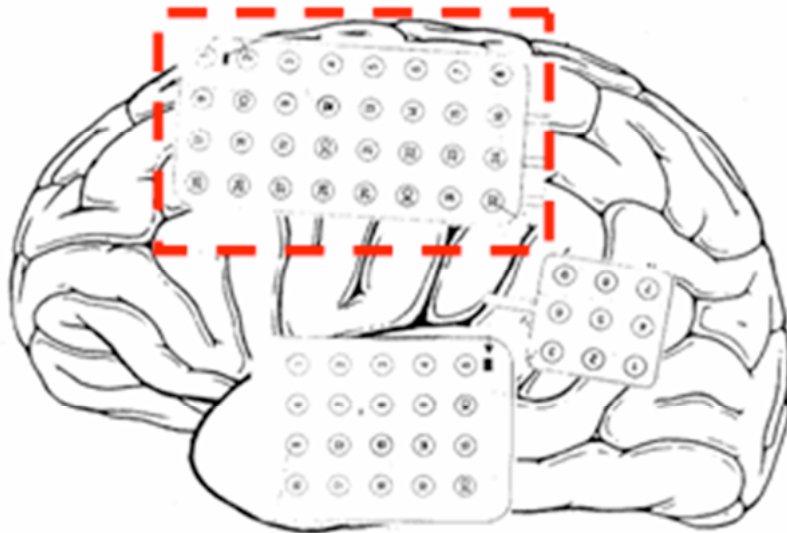


Fig. 1.02. The locations are shown of typical placements by neurosurgeons of arrays of 4 mm diameter electrodes 1 cm apart on the pial surface of neocortex, here shown as the left side of the cerebrum, to record ECoG. From Sanchez, Carney and Principe (2006)

What, then, are the optimal space and time windows in which to construct the space-time averages to extract patterns of successive states as frames without loss of crucial detail? Available evidence (Freeman, 2005a, 2006) shows that frames are not and need not be synchronized with each other, because emergent frames at mesoscopic and macroscopic levels often overlap, possibly by superposition, and possibly by nonlinear interaction. Each mesoscopic frame can be conceived to shape the continuous trajectories of microscopic neural activity that control limb movement by evolving in frames that within themselves appear to be linear and stationary. That patterning of itinerant trajectories (Tsuda, 2001) is extracted and reconstructed using multivariate linear techniques (e.g., Hochberg et al., 2006). The requirements for high-density recording arrays, high-speed digitizing, and linear systems analysis are met; the need now is for comprehensive theory by which to guide decomposition of signals to extract optimized state variables in frames.

4. Size of spatial frames: two modes of description of behavior in BCI

The motor control operations of brains are described from two viewpoints of the simplest experiment: a hungry rat pressing a switch for a pellet, which serves as an animal model for a human subject performing a more complex task. The first viewpoint is that of the behaviorist and engineer, who treat the brain as a deterministic signal generator that can be controlled by reinforcement learning

(Ferster and Skinner, 1957). In behaviorist terms a rat is conditioned to use its forelimb to press a lever (an “operant”) and get a reward or avoid punishment in reinforcement learning (Ohl, Scheich and Freeman, 2001). The behavior of the animal is “shaped” to perform a conditioned response (CR). Next the food is given only when a conditioned stimulus (CS) such as a tone or light flash is paired in a fixed schedule of reinforcement. An array of implanted microelectrodes is used to record the MSA, which samples the cortical activity pattern that mediates the CS into the CR. When the subject has learned the association and can perform the task reliably, the lever is disconnected from the switch controlling the reinforcement, and the MSA is used to deliver it instead. After training is completed, the lever is removed, and the rat performs by using its brain activity through an electronic channel. Successful transfer of reinforcement delivery from an operant to its neural correlate opens a BCI channel.

The second viewpoint is that of the psychologist and pragmatist, who treat the brain as a self-organizing system that predicts its own goals and plans its actions to achieve them. In pragmatist terms the CR is performed through an intentional process that is called the “action-perception cycle”, which is aimed to achieve “maximum grip” (Merleau-Ponty, 1945). The expectation of performing an action to receive a reward such as juice emerges as an internally generated macroscopic intentional state involving thirst by which the rat predicts its future of getting a reward. The initial training (shaping) shapes in the brain the microscopic synaptic connections that the rat must have in order to predict, plan and construct the neural command that executes the forthcoming intentional act of lever pressing with the expectation that reward will follow. This mesoscopic command has the form of oscillatory patterns of dendritic waves and axonal pulses that are embedded in and constrained by the macroscopic state. Each command further constrains the trajectories of spikes that descend into the brain stem and spinal cord. They are accompanied by other patterns of spikes called “corollary discharges” (Sperry, 1950) and “efference copies” (von Holst and Mittelstädt, 1950) that propagate through the brain (not the through the body in the proprioceptive “sixth sense”, Abbott, 2006) to the primary sensory areas. Corollary discharges modify the sensory cortices by conditioning (shaping) their synaptic sensitivities to embody the predictions of the changes in sensory input that will result from acts to search for and consume juice. Then cortical neurons can respond selectively to a CS that is expected, even when it is obscured by noise and distorted by variations in body position. This selective cortical sensitization is called prefference (Kay and Freeman, 1998); it implements attention and expectancy.

The prediction of a range of possible outcomes of each act in search of reward is mediated by the dynamics of the sensory cortices. The selective sensitivities of each sensory cortex form a landscape of basins of attraction (Skarda and Freeman, 1987). Each class of discriminated input corresponds to a learned attractor. The cortex in the expectant state of search has wave and pulse state variables that trace a trajectory through the high-dimensional state space of cortical dynamics. At each time step the cortical state advances by a measurable Euclidean distance

through state space. When an action such as a sniff or a foveation is taken, the afferent spikes that are triggered by a CS in sensory receptors are carried by relays to sensory cortex. The impact of the background noise that accompanies the CS destabilizes the cortex and actualizes the attractor landscape. The CS in the sensory noise selects a basin of attraction, which is one among the sensitized patterns that are potentiated by prefference in the sensory cortex to which the afferent spikes are directed. The trajectory defined by the state variables of the sensory cortex in the high-dimensional hyperspace gives immediate access to any among all basins of attraction, which individually are in low-dimensional subspaces. Capture by a basin initiates the construction of a spatially distributed signal that signifies the class to which the stimulus is assigned. The mesoscopic output pattern transmits the knowledge about the CS from past experience.

Every sensory cortex simultaneously diverges its mesoscopic output, and all outputs converge in the superficial entorhinal cortex, which cycles the combined activity through the hippocampal system where spatial and temporal orientation are assigned to the multisensory percept (Gestalt) in the cognitive map and short term memory. The output from the deep entorhinal cortex diverges to all sensory areas and the pre-motor and motor cortex. A sequence of macroscopic patterns emerge that incorporate all of the areas (Freeman and Burke, 2003; Freeman and Rogers, 2003). By hypothesis the macroscopic pattern embeds an appropriate neural command that evolves by successive mesoscopic frames under the guidance of the surrounding areas in constant communication. That command is accompanied by its observable neural correlates in MSA, LFP and local ECoG. Minimally, that motor correlate is observed in the sensorimotor cortex, measured, and used by the experimentalist to deliver the reward, after disabling the lever-reward connection. Optimally, much of the configuration of the anticipatory corollary discharge of prefference and sensory testing by proprioceptive feedback may be available in the prefrontal, parietal, temporal and occipital cortices in the signals from areas that surround the sensorimotor cortex. The distribution of sampling of mesoscopic and macroscopic cortical activity is profitably quite wide indeed, as shown by Nicolelis (2003) with MSA and by Gao et al. (2003) with EEG.

These two modes of description, the reflex arc starting with a stimulus and the action-perception cycle starting with intention, are not in conflict. Each has its advantages and limitations; they are complementary. They should both be used to define and measure the properties of neural correlates of actions. The behaviorist approach focuses on the movement execution by control in the motor and premotor cortices in the posterior frontal lobe and the proprioceptive feedback of limb movement in the somatosensory cortex in the anterior parietal lobe. The pragmatist approach focuses on the neural context in which the act is performed, including the predictions formulated by the animal and the preparations required of the body in order to perform reliably and robustly. Virtually all structures in the brain are involved in this broad context (Kozma, Freeman and Erdí, 2003; Freeman and Burke, 2003; Freeman and Rogers, 2003; Houk, 2005).

5. Sequential time frames of the neural processing mediating CS into CR

In behaviorist terms the reflex stimulus-response model is constructed with data from spike recording at the microscopic level of analysis. Each trial after training begins with delivery by the investigators of a discriminative CS to the eyes or ears, where the stimulus energy is transduced to spikes and the stimulus information is encoded in spike rates and intervals for transmission to the primary sensory cortex, with pre-processing at spinal and thalamic relays in the ascending path. Cortical networks extract the information by feature detector neurons, bind its features (Singer and Gray, 1995) and send the new spike pattern to association areas for comparison with information already stored by training in associational networks. After identification and classification, the deciding information is sent as yet another a pattern of spikes to the premotor and motor cortices. A motor command is organized by neural modules that include the basal ganglia and cerebellum (Houk and Wise, 1995; Houk, 2005). The command is sent as a spatiotemporal pattern of spikes into the brain stem and spinal cord. The activated limb sends proprioceptive signals to the parietal somatosensory areas, which are selectively activated and integrated into the activity of motor areas. The command patterns are intercepted by arrays of microelectrodes in BCI, and the trial is completed after delivery of the reward. These sequential patterns are inferred to have start and end times giving their durations as well as their spatial locations and sizes. They may well be overlapping and interactive.

In pragmatist terms the nonlinear neurodynamics paradigm is pursued with data from LFP and ECoG at the mesoscopic level of analysis. Each trial after training begins with an expectant state of a rat by which the brain holds the sensory cortices in receiving mode by preaffference. Its intentional stance includes an appropriate posture of head, trunk and limbs (Stuart, 2005) for stabilization of its center of gravity and orientation of its sense organs to the expected types and locations of CS. Preparation for action also includes optimization of the janitorial functions of the autonomic and neuroendocrine back-up systems. Attention is focused through preaffference by construction of relevant attractor landscapes in all sensory cortices. The basins of attraction in each landscape (Skarda and Freeman, 1987; Kozma and Freeman, 2001) include selective sensitivities to the background inputs that the rat continually checks to detect all expected discriminative CS. Each attractor landscape also includes the basin of an attractor for novel or unexpected stimuli, which generates unpatterned “chaotic” activity that evokes an orienting response to a salient unknown stimulus and enables the formation of new attractors by Hebbian category learning (Ohl, Scheich and Freeman, 2001). While the rat is attentive and expectant, holding its cortices in open receptive mode, it is ready to receive a CS.

Sensory receptors respond to whatever they receive; habituation is cortical. Each CS is embedded in background noise. The impact on each sensory cortex of the afferent spikes evoked by background greatly exceeds that of the CS and

destabilizes the cortex. The state transition is a spontaneous symmetry breaking (Freeman and Vitiello, 2006) that activates the latent attractor landscape in each primary sensory cortex. The ECoG reflects an intracortical search trajectory in n -space by which the sensory information in the spikes selects an appropriate basin of attraction. Each attractor is based in a Hebbian cell assembly of mutually excitatory pyramidal cells. The spikes specifically evoked by the CS excite the cells in one assembly, which amplify the impact and result in the selection of that assembly and attractor. On convergence of the intracortical search trajectory to the selected low-dimensional attractor, each sensory cortex in its transmitting mode broadcasts a spike pattern that designates the class to which the cortex has assigned the CS, and it incrementally modifies and updates the selected attractor in the continuing process of learning. Convergence to the attractor implements the process of generalization (Lashley, 1942). The cortex deletes the raw sensory information during transmission. Smoothing imposed by a spatiotemporal integral transform in the output pathway implements the process of abstraction (Freeman, 2004a,b, 2005, 2006).

The description in terms of sparse networks of neurons in Hebbian assemblies that communicate by spike trains is microscopic. The description in terms of neural populations, spike densities in MSA, dendritic current densities in LFP from microwires, and local ECoG from a pial surface array is mesoscopic. The behavioral description and use of the electroencephalogram (EEG) from the scalp as well as other tools for imaging (MEG, fMRI, etc.) is macroscopic. Again, these descriptions are complementary, because they address different hierarchical levels of brain function. The state variables at the microscopic level are measured in the pulse trains, which must be averaged in one way or another for correlation with the state variables at the mesoscopic level. The field potentials measured at that level must be combined and expressed as high dimensional feature vectors for correlations with the behavior that is measured at the macroscopic level. Multidimensional scaling and statistics project high dimensional clusters into 2-D for visualization and classification (Freeman and Grajski, 1987; Barrie et al., 1999).

There are two salient aspects of MSA feature vectors in the pulse mode that help predict the relevant LFP and ECoG feature vectors in the wave mode. One is the success of empirical temporal coarse-graining of spike activity into 50-250 ms bins. This produces a time-to-amplitude conversion that is critical for adaptive filters that correlate modulations in amplitude. The other is the spatial patterning of mean pulse densities of the multichannel MSA feature vector in each time step (Carmena et al., 2006). The counterparts in the accompanying LFP and ECoG in the wave mode are revealed by decomposing the LFP and ECoG signals respectively into the gain and phase at each frequency by means of the Fourier transform (Barrie, Freeman and Lenhart, 1996; Freeman and Barrie, 2002) at each digitizing step. Each signal has multiple rates of change seen in the power law ($1/f^\alpha$) distribution of energy density in power spectral densities (PSD) of brain field potentials (Freeman et al., 2003; Freeman, 2006). The highest power is in the

empirical theta (3-7 Hz) and alpha (8-12 Hz) ranges, followed by the beta (12-30 Hz) and gamma (30-80 Hz) ranges. Beta and gamma rates reflect the carrier frequencies of spatial patterns of amplitude modulation in frames; theta and alpha rates reflect the frame repetition rates. Higher frequencies form the epsilon range of 80 to 300 Hz. Beta β and gamma γ oscillations (Bressler and Freeman, 1980) result from negative feedback with time constants near 5 ms giving center frequencies near 40 Hz (Freeman, 1975/2000), whereas epsilon ϵ oscillations reflect positive feedback (pp. 181 ff. in Freeman, 2000) again with time constants near 5 ms but with maximal center frequencies near 200-250 Hz. The highest range, >300 Hz in ECoG from surface electrodes (Fig. 1.02) as well as LFP from depth electrodes, manifests massed multiunit activity (MUA) from innumerable action potentials that merge into fluctuations that resemble thermal noise, which can contribute a behavioral correlate by variations in its root mean square (rms) amplitude. The fluctuations would be indistinguishable from thermal noise were it not for low-frequency variations in mean amplitude correlated with behavior as seen in spatial displays. MUA activity resembles muscle potentials (electromyogram, EMG) in having a flat spectrum with low frequencies in the envelope, and in being measurable only at high temporal frequencies. This is because the $1/f^\alpha$ amplitude spectrum enables ECoG and LFP to dominate at low temporal frequencies and EMG and MUA to appear at high temporal frequencies.

6. A hypothesis: Five steps in the central dynamics mediating CS into CR

John von Neumann (1958) wrote: “Whatever the language of the brain is, it cannot fail to differ considerably what we consciously and explicitly consider as mathematics Brains lack the arithmetic and logical depth that characterize our computations. . . . We require exquisite numerical precision over many logical steps to achieve what brains accomplish in very few short steps” (pp. 80-81). We are now in a position to describe in non-mathematical terms five central “short steps” in a sequence major state transitions that give a kind of scaffold for analysis of the action-perception cycle: downwardly from macrostates to microstates and upwardly in the reverse direction. According to this hypothesis training establishes a macroscopic state at the beginning of a trial, which is expressed in a global pattern of forebrain activity constituting a state of understanding, attention, and preparedness. 1. That pattern supports formation by state transition of a prediction of some future state by extrapolation based in experience. The mechanism is unknown. 2. The new macroscopic pattern embeds and constrains multiple mesoscopic patterns that appear as locally coherent domains of neural activity implementing planning and preference. 3. Each local pattern constrains the neurons in the domains, inducing them to form microscopic patterns of spike activity and transmit them into the brain stem, spinal cord, and other cortices. Outside the brain the body executes an act including observation. The occurrence of an expected event triggers transmission of a barrage of spikes to the sensory cortices. 4. In each cortex a state transition enables the emergence of a mesoscopic pattern that constrains the transmitting neurons into a spike pattern that is broadcast to other parts of the brain including the limbic system. 5.

According to this hypothesis the integration of activity from multiple areas through the limbic system precipitates a macroscopic state transition to a new spatial pattern that replaces and updates the preexisting pattern, closing the cycle.

Classical and operant conditioning studies of sensory cortical activity have yielded the data needed to construct this hypothesis by extrapolation from the sensory-perceptual limb. BCI offers an opportunity to test the five-step hypothesis by revealing the way in which macroscopic patterns of brain activity precede and guide the formation first of mesoscopic patterns and then of spatial patterns of MSA and trajectories of limb movements. The strategy that is proposed in Part 2 is linear decomposition of ECoG, identification of the spatial and temporal locations (start and end times) of individual frames, and application of linear analysis and multivariate statistics for classification of frames with respect to behavior, so that within each frame the time-dependent trajectory of MSA that relates to limb movement might be described. An analogy from the field of engineering is flight control of an aircraft. An operator selects the end point of a flight plan. An outer loop controller expresses the plan in a series of set points. A set of inner loop controllers adjusts the control surfaces of the aircraft to maintain the inputs of flight sensors within designated ranges. The thrust of the analogy is that using MSA tends to focus on the details of limb control, whereas using ECoG and LFP may give access to higher order expressions of goal states and their derivatives, by which the brain selects among its modules the interactive patterns needed construct limb trajectories and adapt them to local adventitious conditions.

7. References

- Abbott A (2006) Neuroprosthetics: In search of a sixth sense. *Nature* 442: 125-127.
- Andersen RA, Snyder LH, Bradley DC, Xing J (1997) Multimodal representation of space in the posterior parietal cortex and its use in planning movements. *Ann. Rev. Neurosci* 20: 303-330.
- Andersen RA, Musallam S, Pesaran B (2004) Selecting the signals for a brain-machine interface. *Curr Opin Neurobiol* 14(6):720-6.
- Abeles M (1991) *Corticonics: Neural Circuits of the Cerebral Cortex*. New York: Cambridge UP.
- Barabási A-L (2002) *Linked. The New Science of Networks*. Cambridge MA: Perseus.
- Barrie JM, Freeman WJ, Lenhart M (1996) Modulation by discriminative training of spatial patterns of gamma EEG amplitude and phase in neocortex of rabbits. *J Neurophysiol* 76: 520-539.
- Barrie JM, Holcman D, Freeman WJ. (1999) Statistical evaluation of clusters derived by nonlinear mapping of EEG spatial patterns. *J Neurosci Meth.* 90: 87-95.
- Basar E (1998) *Brain Function and Oscillations. 1. Principles and Approaches. 2. Integrative Brain Function, Neurophysiology and Cognitive Operations*. Berlin: Springer-Verlag.
- Blanche TJ, Spacek MA, Hetke JF, Swindale NV (2005) Polytrodes: high-density silicon electrode arrays for large-scale multiunit recording. *J Neurophysiol.* 93(5): 2987-3000.
- Blankertz B, Mueller KR, Curio G, Vaughan TM, Schalk G, Wolpaw JR, Schloegl A, Neuper C, Pfurtscheller G, Hinterberger T, Schoeder M, Birbaumer M. (2004) The BCI Competition 2003: Progress and perspectives in detection and discrimination of EEG single trials. *IEEE Trans Biomed Engin* 51: 1044-1051.
- Bok ST (1959) *Histonomy of the Cerebral Cortex*. Amsterdam: Elsevier.
- Braitenberg V, Schüz A (1998) *Cortex: Statistics and Geometry of Neuronal Connectivity*, 2nd ed. Berlin: Springer-Verlag.
- Bressler SL, Freeman WJ (1980) Frequency analysis of olfactory system EEG in cat, rabbit and rat. *Electroencephalogr clin Neurophysiol* 50: 19-24.
- Bressler SL, Kelso JAS (2001) Cortical coordination dynamics and cognition. *Trends Cogn Sci* 5: 2-36.
- Carmena JM, Lebedev MA, Crist RE, O'Doherty JE, Santucci DM, Dimitrov DF, Patil PG, Henriquez CS, Nicolelis MAL (2003) Learning to control a brain-machine interface for reaching and grasping by primates. *PLoS Biology* 1:193-208.
- Carmena JM, Lebedev MA, Henriquez CA, Nicolelis MAL (2005) Stable ensemble performance with single-neuron variability during reaching movements in primates. *J Neuroscience* 25(46): 10712-10716.

- Chapin JK, Moxon KA, Markowitz RS, Nicolelis MAL (1999) Real-time control of a robot arm using simultaneously recorded neurons in the motor cortex. *Nature Neurosci* 2: 664-670.
- Cheng M, Gao X, Gao S, Xu D (2002) Design and implementation of a brain-computer interface with high transfer rates. *IEEE Trans Biomed Eng* 49(10): 1181-1186. SSVEP
- Cohen D, Nicolelis MAL (2004) Reduction of single-neuron firing uncertainty by cortical ensembles during motor skill learning. *J Neurosci* 24: 3574-3582.
- DiGiovanna J, Sanchez JC, Principe JC (2006) Improved linear BMI systems via population averaging. *Proc. EMBS*.
- Donoghue JP (2002) Connecting cortex to machines: recent advances in brain interfaces. *Nat Neurosci. Suppl*:1085-8.
- Ferster CB, Skinner BF (1957) *Schedules of Reinforcement*. Englewood Cliffs NJ: Prentice-Hall.
- Fingelkurts AnA, Fingelkurts AIA (2004) Making complexity simpler: multivariability and metastability in the brain. *Int J Neurosci* 114: 843-862.
- Freeman WJ (1975) *Mass Action in the Nervous System*. New York: Academic.
- E-format (2004): <http://sulcus.berkeley.edu/MANSWWW/MANSWWW.html>
- Freeman WJ (1979) Nonlinear gain mediating cortical stimulus-response relations. *Biological Cybernetics* 33:237-247.
- Freeman WJ (2000) *Neurodynamics: An Exploration of Mesoscopic Brain Dynamics*. London: Springer.
- Freeman WJ (2004a) Origin, structure, and role of background EEG activity. Part 1. Analytic amplitude. *Clin Neurophysiol* 115: 2077-2088.
- Freeman WJ (2004b) Origin, structure, and role of background EEG activity. Part 2. Analytic phase. *Clin Neurophysiol* 115: 2089-2107.
- Freeman WJ (2005a) Origin, structure, and role of background EEG activity. Part 3. Neural frame classification. *Clin Neurophysiol*. 116 (5): 1118-1129.
- Freeman WJ (2005) A field-theoretic approach to understanding scale-free neocortical dynamics. *Biol Cybern* 92/6: 350-359.
- Freeman WJ (2006) Origin, structure, and role of background EEG activity. Part 4. Neural frame simulation. *Clin Neurophysiol* 117: 572-589.
- Freeman WJ, Burke BC (2003) A neurobiological theory of meaning in perception. Part 4. Multicortical patterns of amplitude modulation in gamma EEG. *Int J Bifurc Chaos* 13: 2857-2866.
- Freeman WJ, Grajski KA (1987) Relation of olfactory EEG to behavior: Factor analysis. *Behav Neuroscience* 101: 766-777.
- Freeman WJ, Rogers LJ (2003) A neurobiological theory of meaning in perception. Part 5. Multicortical patterns of phase modulation in gamma EEG. *Int J Bifurc Chaos* 13: 2867-2887.
- Freeman WJ, Rogers LJ, Holmes MD and Silbergeld DL (2000) Spatial spectral analysis of human electrocorticograms including the alpha and gamma bands. *J Neurosci Meth* 95: 111-121.
- Freeman WJ, Vitiello G (2006) Nonlinear brain dynamics as macroscopic manifestation of underlying many-body field dynamics. *Physics Life Reviews* 3: 93-118.

- Gao X, Xu D, Cheng M, Gao S (2003) A BCI-based environmental controller for the motion-disabled. *IEEE Trans Rehab Engin* 11(2): 137-140.
- Georgopoulos AP, Schwartz AB, Kettner RE (1986) Neuronal population coding of movement direction. *Science* 233: 1416-1419.
- Gonzalez SL, Grave de Peralta R, Thut G, Millán J del R, Morier P, Landis T (2006) Very high frequency oscillations (VHFO) as a predictor of movement intentions. *NeuroImage*, Short Communication, in press.
- Granit R, Kernell D, Shortess GK (1963) Quantitative aspects of repetitive firing of mammalian motoneurons caused by injected currents. *J Physiol* 168: 453-472.
- Granit R, Renkin B (1961) Net depolarization and discharge rate of motoneurons, as measured by recurrent inhibition. *J Physiol* 158: 461-475.
- Haken H (1983) *Synergetics: An Introduction*. Berlin: Springer-Verlag.
- Hinterberger T, Kubler A, Kaiser J, Neumann N, Birbaumer N (2003) A brain-computer interface (BCI) for the locked-in: comparison of different EEG classifications for the thought translation device. *Clin Neurophysiol* 114: 416-425.
- Hochberg LR, Serruya MD, Friehs GM, Mukand JA, Saleh M, Caplan AH, Branner A, Chen D, Penn RD, Donoghue JP (2006) Neuronal ensemble control of prosthetic devices by a human with tetraplegia *Nature* 442: 164-172.
- Houk JC (2005) Agents of the mind. *Biol Cybern* 92: 427-437.
- Houk JC, Wise SP (1995) Distributed modular architectures linking basal ganglia, cerebellum, and cerebral cortex: Their role in planning and controlling action. *Cerebral Cortex* 5: 95-110.
- Kay LM, Freeman WJ (1998) Bidirectional processing in the olfactory-limbic axis during olfactory behavior. *Behav Neurosci* 112: 541-553.
- Kipke DR, Vetter RJ, Williams JC (2003) Silicon-substrate intracortical microelectrode arrays for long-term recording of neuronal spike activity in cerebral cortex. *IEEE Trans Rehab Engin* 11: 151-155.
- Kozma R, Freeman WJ (2001) Chaotic resonance: Methods and applications for robust classification of noisy and variable patterns. *Intern J Bifurc Chaos* 10: 2307-2322.
- Kozma R, Freeman WJ and Erdí P (2003) The KIV model – nonlinear spatiotemporal dynamics of the primordial vertebrate forebrain. *Neurocomputing* 52: 819-826.
- Kozma R, Puljic M, Balister P, Bollobas B, Freeman WJ (2004) Neuropercolation: A random cellular automata approach to spatiotemporal neurodynamics. Ch. in: *Lecture Notes in Computer Science*: 141.225.40.170 springerlink.com
<http://repositories.cdlib.org/postprints/1013>.
- Lashley KS (1942) The problem of cerebral organization in vision. In: Cattell J (ed.) *Biological Symposia VII*: 301-322.
- Lee D, Port NL, Kruse W, Georgopoulos AP (1998) Variability and correlated noise in the discharge of neurons in motor and parietal areas of the primate cortex. *J Neurosci* 18: 1161-1170.

- Li X, Li G, Wang L, Freeman WJ (2006) A study on a bionic pattern classifier based on olfactory neural system. *Int J Bifurc Chaos*, in press.
- Liley DTJ, Wright JJ (1994) Intracortical connectivity of pyramidal and stellate cells: estimates of synaptic densities and coupling symmetry. *Network* 5: 175-189.
- Mehring C, Rickert J, Vaadia E, Cardoso de Oliveira S, Aertsen A, Rotter S (2003) Inference of hand movements from local field potentials in monkey motor cortex. *Nature Neurosci* 6(12): 1253-1254.
- Merleau-Ponty M (1945/1962) *Phenomenology of Perception*. (C Smith, Trans.). New York: Humanities Press.
- Millay J (1999) *Multidimensional Mind: Remote Viewing in Hyperspace*. Berkeley CA: North Atlantic Books.
- Miltner WHR, Barun C, Arnold M, Witte H, Taub E (1999) Coherence of gamma-band EEG activity as a basis for associative learning. *Nature* 397: 434-436.
- Müller MM, Bosch J, Elbert T, Kreiter A, Valdes Sosa M, Valdes Sosa P, Rockstroh B (1996) Visually induced gamma band responses in human EEG - A link to animal studies. *Exper Brain Res* 112: 96-112.
- Musallam S, Corneil BD, Greger B, Scherberger H, Andersen RA (2004) Cognitive control signals for neural prosthetics. *Science* 305:258-262.
- Nicolelis MAL (2001) Actions from thoughts. *Nature* 409: 403-407.
- Nicolelis MA (2003) Brain-machine interfaces to restore motor function and probe neural circuits. *Nat Rev Neurosci*. 4(5):417-22.
- Nunez PL, Srinivasan R, Westdorp AF, Wijesinghe RS, Tucker DM, Silberstein RB, Cadusch PJ (1997) EEG coherency I: statistics, reference electrode, volume conduction, Laplacians, cortical imaging and interpretation at multiple scales. *Electroenceph clin Neurophysiol* 103: 499-515.
- Ohl FW, Scheich H, Freeman WJ (2001) Change in pattern of ongoing cortical activity with auditory category learning. *Nature* 412: 733-736.
- Othmer S, Othmer SF, Kaiser DA (1999) EEG biofeedback: an emerging model for its global efficacy. Ch. 11 in: Evans JR, Abarbanel A (eds.) *Introduction to Quantitative EEG and Neurofeedback*. New York: Academic, pp. 243-310.
- Prigogine I (1980) *From Being to Becoming: Time and Complexity in the Physical Sciences*. San Francisco: W H Freeman.
- Principe JC, Tavares VG, Harris JG, Freeman WJ (2001) Design and implementation of a biologically realistic olfactory cortex in analog VLSI. *Proc IEEE* 89: 1030-1051.
- Rodriguez E, George N, Lachaux J-P, Martinerie J, Renault B, Varela F (1999) Perception's shadow: long-distance synchronization of human brain activity. *Nature* 397: 430-433.
- Sanchez JS, Carmena JM, Lebede MA, Nicolelis MAL, Harris JG, Principe JC (2004) Ascertaining the importance of neurons to develop better brain-computer interfaces. *IEEE Trans Biomed Eng* 51: 943-953.
- Sanchez JS, Carney PR, Principe JC (2006) Analysis of amplitude modulated control features for ECoG neuroprosthetics. *IEEE Intern Conf Engin Biol Med*, in press.

- Schroeder M (1991) *Fractals, Chaos, Power Laws*. San Francisco: WH Freeman.
- Serruya MD, Hatsopoulos NG, Paninski L, Fellows MR, Donoghue JP (2002) Instant neural control of a movement signal. *Nature* 416: 141-142.
- Sholl DW (1956) *The Organization of the Cerebral Cortex*. New York: Wiley.
- Singer W, Gray CM (1995) Visual feature integration and the temporal correlation hypothesis. *Ann Rev Neurosci* 18: 555-586.
- Skarda CA, Freeman WJ (1987) How brains make chaos in order to make sense of the world. *Behav Brain Sci* 10: 161-195.
- Sperry RW (1950) Neural basis of the spontaneous optokinetic response. *J Comparative Physiology* 43: 482-489.
- Stuart DG (2005) Integration of posture and movement: Contributions from Sherrington, Hess and Bernstein. *Human Movement Sci* 24: 621-643.
- Swadlow HA (1994) Efferent neurons and suspected interneurons in motor cortex of the awake rabbit: axonal properties, sensory receptive fields and subthreshold synaptic inputs. *J Neurophysiol* 71: 437-453.
- Tallon-Baudry C, Bertrand O, Delpuech C, Pernier J (1996) Stimulus-specificity of phase-locked and non phase-locked 40-Hz visual responses in human. *J Neurosci* 16: 4240-4249.
- Tallon-Baudry C, Bertrand O, Peronnet F, Pernier J (1998) Induced gamma-band activity during the delay of a visual short-term memory task in humans. *J Neurosci* 18: 4244-4254.
- Taylor DM, Tillery SI, Schwartz AB (2002) Direct cortical control of 3D neuroprosthetic devices. *Science* 296: 1829-1832.
- Tsuda I (2001) Toward an interpretation of dynamics neural activity in terms of chaotic dynamical systems. *Behav Brain Sci* 24: 793-847.
- Von Holst E, Mittelstädt H (1950) Das Reafferenz Prinzip. Wechselwirkung zwischen Zentralnervensystem und Peripherie. *Naturewissenschaften* 37: 464-476.
- von Neumann J (1958) *The Computer and the Brain*. New Haven CT: Yale UP.
- Wang Y, Sanchez JC, Principe JC, Mitzelfelt JD, Gunduz A (2006) Analysis of the correlation between local field potentials and neuronal firing rate in the motor cortex. *Proc EMBS*.
- Wessberg J, Stambaugh CR, Kralik JD, Beck PD, Laubach M, Chapin JK, Kim J, Biggs SJ, Srinivasan MA, Nicolelis MAL (2000) Real-time prediction of hand trajectory by ensembles of cortical neurons in primates. *Nature* 408:361-365.

Appendix 1. Wave-pulse statistical relations.

A continuous record is digitized at 1 KHz simultaneously of a spike train of a single neurons and the ECoG at the cortical site of penetration (Freeman, 1975/2004). The ECoG is filtered in the pass band of the desired oscillatory frequency, e.g., 20-80 Hz. The spike train is accumulated to give $n_p \sim 10,000$ pulses expressed as a series of 0's and 1's. The N values of ECoG values are normalized to zero mean and unit SD; an amplitude histogram is divided into 61 bins centered at 0 and ranging between ± 3 SD in steps of 0.1 SD. At each time step the question is asked, is there a pulse in any bin between $T = 0$ and $T = \pm T_r$ time steps (e.g., $T_r = \pm 25$ ms preceding and following $T = 0$ ms). A 1-D table of the pulse occurrences at each amplitude is accumulated at $T = 0$, $p(v)$. The $n_v(v)$ values in each bin, n_v , are divided by the total number of pairs to get the probability density for amplitude at $T = 0$:

$$P(V) = n_v(v) / N. \quad (A1.1)$$

The number of pulses in each bin, $n_p(p, v)$ is divided by the total number of pairs to give the joint pulse-amplitude probability density at $T = 0$:

$$P(p \cap v) = n_p(p, v) / N. \quad (A1.2)$$

The pulse probability density is divided by the amplitude probability density to give the pulse probability conditional on amplitude at $T = 0$:

$$P(p|v) = P(p \cap v) / p(v). \quad (A1.3)$$

The algorithm is repeated at each time lag between $-T_r$ and $+T_r$ to get the pulse probability conditional on time and amplitude in 2-D, which is then normalized by dividing the function by the grand mean pulse probability, P_o :

$$P(p|T \cap v) = P(p \cap T \cap v) / p(v). \quad (A1.4)$$

The function is normalized by dividing all values by the grand mean pulse probability, P_o to get the normalized conditional pulse probability (NCPD):

$$P_n(p|T \cap v) = P(p|T \cap v) / P_o. \quad (A1.5)$$

The time dependence of the NCPD is found by averaging across the upper third of the range for $v > 0$, giving the pulse probability wave that is comparable to the autocorrelation of the filtered ECoG or LFP:

$$P_{n,v}(T) = 1/k \sum P_n(p|T \cap v), \quad SD \leq v_k \leq 3 SD. \quad (A1.6)$$

The sigmoid curve is the NCPD on amplitude is estimated by averaging over lag times at k values where the deviation of $P_v(T)$ above zero is maximal:

$$P_{n,t}(v) = 1/k \sum P_n(p|T \cap v), \quad P(T_k) \gg P_o. \quad (\text{A1.7})$$

The sigmoid curve is fitted to the data (Fig. 1.01, A) in order to evaluate the upper asymptote, Q_m , as given in the equation inset with the data. The asymptote varies in proportion to the degree of arousal, and it has differing mean values for differing populations in the olfactory and limbic systems. The forward gain of the population is given by the derivative of the sigmoid curve, dq/dv . Two examples are shown for $Q_m = 2$ in behavioral rest and $Q_m = 5$ in arousal (Freeman, 2000) for comparison with the numerical derivative in Fig. 1.01, A. The maximal gain, $v_{\max} = \ln Q_m$ from the second derivative set to 0, is displaced to the excitatory side. This asymmetry underlies the input-dependent nonlinearity of cortical dynamics, which is required for the destabilization in spontaneous breaking of symmetry by state transitions (Freeman and Vitiello, 2006). From Freeman (1979; reprinted Ch. 10, 2000)